

Automotive FMCW Radar-enhanced Range Estimation via a Local Resampling Fourier Transform

Regular Paper

Cailing Wang^{1*}, Huajun Liu², Guang Han¹ and Xiaoyuan Jing¹

¹ Nanjing University of Posts and Telecommunications, Nanjing, China

² Nanjing University of Science and Technology, Nanjing, China

*Corresponding author(s) E-mail: wangcl@njupt.edu.cn

Received 14 October 2015; Accepted 20 December 2015

DOI: 10.5772/62179

© 2016 Author(s). Licensee InTech. This is an open access article distributed under the terms of the Creative Commons Attribution License (<http://creativecommons.org/licenses/by/3.0/>), which permits unrestricted use, distribution, and reproduction in any medium, provided the original work is properly cited.

Abstract

In complex traffic scenarios, more accurate measurement and discrimination for an automotive frequency-modulated continuous-wave (FMCW) radar is required for intelligent robots, driverless cars and driver-assistant systems. A more accurate range estimation method based on a local resampling Fourier transform (LRFT) for a FMCW radar is developed in this paper. Radar signal correlation in the phase space sees a higher signal-noise-ratio (SNR) to achieve more accurate ranging, and the LRFT - which acts on a local neighbour as a refinement step - can achieve a more accurate target range. The rough range is estimated through conditional pulse compression (PC) and then, around the initial rough estimation, a refined estimation through the LRFT in the local region achieves greater precision. Furthermore, the LRFT algorithm is tested in numerous simulations and physical system experiments, which show that the LRFT algorithm achieves a more precise range estimation than traditional FFT-based algorithms, especially for lower bandwidth signals.

Keywords Automotive Radar, FMCW, Range Estimation, Phase Correlation, Local Resampling Fourier Transform

1. Introduction

Automotive millimetre-wave (MMW) frequency-modulated continuous-wave (FMCW) radars are generally used in diverse applications owing to their low cost, simplicity and robustness in foggy, rainy, dusty and humid conditions [1, 2], and they are often configured as medium-range and long-range radars for intelligent robots, driverless cars and driver-assistant systems [3]. These radars have also been used in ground and maritime surveillance tasks for the detection and tracking of targets [4, 5].

High-performance automotive radar systems have been available on the market at 77 GHz; furthermore, an accurate and high-resolution target range and velocity can be measured simultaneously, even in multi-target situations. It is a specific task for a radar to measure a single object's range and radial velocity simultaneously within a single measurement cycle. A single pulse is transmitted and received to measure the range. A continuous wave (or pulse-Doppler) radar is used to measure the radial velocity. In order to measure the range and radial velocity simultaneously within a single measurement cycle, waveforms such as FMCW, mono-pulse, multiple frequency shift keying (MFSK), frequency shift keying (FSK) and chirp sequence (CS) [6] are usually adopted in automotive radar.

A typical approach to measure the range and velocity is to analyse the Fourier spectrum of the received beat signal in FMCW radar. The convolution of the received signal and the transmitted signals is usually used to reach the Fourier spectrum. However, precise range measurement is possible when caused by signal delay, which is determined by the number of samples, the ADC sampling rate, the signal bandwidth and the chirp period, while at the same time the Doppler frequency estimation's precision determines the velocity measure's accuracy [7]. As such, the estimated accuracy of the range and velocity is limited.

The frequency of the beat-note signal is the basis of the range estimation for FMCW-level radar. The instantaneous phase of the sampled series is calculated and is then used to estimate the frequency of a single-tone – however, phase unwrapping is needed to eliminate any ambiguity [8]. To achieve good performance for the ranging in a low Signal Noise Ratio (SNR) situation, frequency estimation techniques employ the correlation algorithm between the sampled data. Frequency estimation algorithms based on the phase difference or the instantaneous phase have to achieve a trade-off between the efficiency of the frequency estimation and its accuracy. In addition, the frequency can be estimated by other methods. In [9, 10], a spectral estimation algorithm based on frequency interpolation for range and velocity enhancement was employed, but the frequency interpolation is based on a nonlinear regression, which is sensitive to the selection of the regression function. FFT is a traditional method for estimating the frequency of signals; however, the duration of the observation limits the estimation accuracy, which is considered to be its obvious drawback. The frequency estimation accuracy can be improved by zero-padded FFT [11], but this will increase the computational burden and demand on memory. Variable sweep time [12] or data oversampling strategies [13] were also used to increase the resolution or sampling precision, which will improve the frequency estimation's precision.

In this paper, we develop an LRFT method for fast and accurate range estimation for an automotive FMCW radar. The method uses the phase correlation technique to achieve a higher SNR pulse compression (PC) spectrum, and then a virtual sample transform is used in a local neighbour around the initial rough estimation to achieve accurate, efficient and robust range parameters. This is a newly developed method of PC using transmitted signals and received signals. The phase correlation-based PC spectrum is used to estimate a rough estimation in order to construct a virtual sample matrix. Then a small region around the rough estimation is transformed by the inverse Fourier transform with a matrix form to achieve a refined delta function. Therefore, we can estimate spectrum peak location and the target's range more precisely. The method works efficiently because of the transformation in the frequency domain by working on a small local neighbourhood and operating as a fast inverse Fourier transform.

The contents of this paper are as follows: in Section 2, we give the FMCW radar's basic range estimation principle. In Section 3, we describe the LRFT method and the developed range estimation algorithm. In Section 4, experimental results are then shown on a simulative platform and a physical system. Finally, a conclusion is given in Section 5.

2. Overview of the FMCW radar and range measuring

A 24 GHz automotive radar is used to measure pedestrians for the evaluation of the proposed algorithm in Section 3. For high-accuracy measurements, the voltage-controlled oscillator (VCO) of the radar must be stabilized with a phase-locked loop (PLL). To minimize the influence of multiple reflections, a parasitic patch antenna in combination with a lens is used as the radar antenna. The radar antenna has an overall gain of 20 dBm and an antenna horizontal beam-width of 23° [14]. As the reference system, the inductive measurement system IVQ-905 K-band VCO antenna by InnoSent Corp. of Germany, which achieves a maximum accuracy of 1 μ m, is used. After the A/D conversion of the beat-frequency signal, the samples are sent to a TMS320F28335 processing unit for online signal processing. To reduce the computing time and minimize the influence of distortion, the beat frequency at each measurement position is calculated by a de-chirp algorithm and the Hamming window.

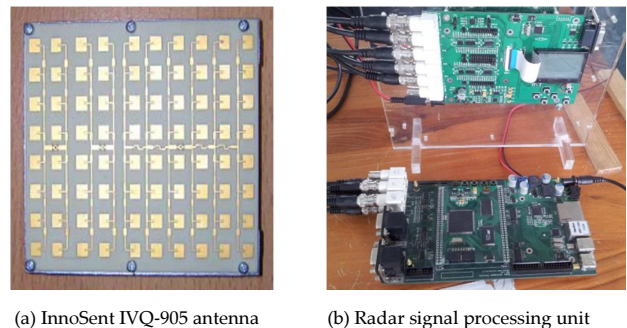


Figure 1. A 24 GHz automotive radar configuration

The range and velocity of a target is estimated by the FMCW radar transmitting a frequency-modulated continuous wave. To a stationary target, frequencies can be described through t_d , the time of the transmitted signal and received signals, as shown in Fig. 2 [15, 16], where f_c is the centre frequency, B is the modulation bandwidth of the signal, and f_0 is the starting frequency. One half of the pulse repetition interval (PRI - also called the chirp period) is described by T .

There will be a Doppler shift in a received signal if it is a moving target, which will be added to the frequency shift caused by t_d . The difference between the transmitted signal and the received signal is the beat frequency; furthermore, the up-chirp and down-chirp beat-frequencies are denoted, respectively, as f_{bu} and f_{bd} . We express f_d (the Doppler

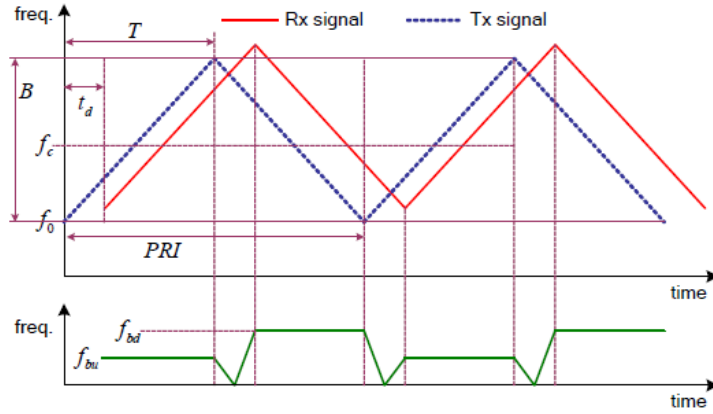


Figure 2. Frequencies of the transmitted, received and beat signals for a moving target

frequency) and f_r (the range beat-frequency) as $f_r = |f_{bu} + f_{bd}|/2$ and $f_d = |f_{bu} - f_{bd}|/2$.

Therefore, f_r and f_d are usually obtained through a signal processing process, and then we can estimate the radial distance and velocity of the target using Equations (1) and (2),

$$R = \frac{CTf_r}{2B} \quad (1)$$

$$V = \frac{Cf_d}{2f_c} \quad (2)$$

where C is the speed of light, B is the modulation bandwidth and T denotes the PRI, which is the chirp period.

The difference between the ideal beat-frequency in the continuous frequency domain and that in the discrete frequency domain in Equation (3) is called the “measure error” of the beat frequency [17]. Here, the ideal beat-frequency is denoted by f_b^{ideal} , the discrete beat-frequency by FFT is denoted by f_b^{FFT} , and we use f_{err} to denote the beat-frequency error, whose maximum error is equal to $\Delta f = f_s/N_s$.

$$f_{err} = f_b^{ideal} - f_b^{FFT} \quad (3)$$

Therefore, the steps for the range and velocity are shown in Equations (4) and (5), respectively. At the same time, the maximum error of the range and velocity are equal to ΔR and Δv , respectively. When a longer chirp is chosen, the step of the velocity will be diminished more; however, the step of the range will be invariant because the fixed frequency step Δf is equal to $1/T$ [18].

The range step ΔR is calculated as shown in Equation (4),

$$\Delta R = \frac{CTf_b}{2B} = \frac{CT}{2B} \cdot \frac{f_s}{N_{FFT}} \quad (4)$$

$$\Delta v = \frac{C\Delta f}{2f_c} = \frac{C}{2f_c} \cdot \frac{f_s}{N_{FFT}} \quad (5)$$

Here, f_s is the analogue-to-digital converter (ADC) sampling rate and N_{FFT} is the FFT point. The maximum PRI is determined by Equation (6).

$$T = 1/(2 \cdot f_{maxD}) \quad (6)$$

In this equation, f_{maxD} is the maximum Doppler frequency to be detected.

3. Accurate range estimation based on the LRFT

In our work, we apply a refinement step to enhance the range estimation after the de-chirp process in the FMCW radar for target detection and range measuring.

Both signals are embedded in a phase space by creating delay vectors. The signal $s(t)$ is the discretely sampled version of the transmitted signal, and $h(t) = s(t + t_0)$ is the signal that has been reflected from some object. If $s(t)$ and $h(t)$ are aligned in time, then the two corresponding signals will be very close in the phase space [19]. Furthermore, the correlation spectrum calculated through the phase space strategy is narrower than the conventional cross correlation method, and the target’s location may be specified with greater precision because the peak location of the spectrum declares the range estimation of the target. Therefore, the correlation in the phase space - rather than in time - is developed. The phase correlation theory is used to calculate the spectrum [20], as shown in Equation (7), where $S(u)$ and $H(u)$ are the Fourier transform signals of $s(t)$ and $h(t)$, respectively, and where $(*)$ denotes complex conjugation and D is the dimension of t . Thus, the cross-correlation in phase space is

$$P_{hs}(u) = \frac{H(u)S^*(u)}{|H(u)S^*(u)|} = \exp\left(-i2\pi\left(\frac{ut_0}{D}\right)\right) \quad (7)$$

The inverse Fourier transform of $P_{hs}(u)$ is the phase correlation spectrum, which is also called PC spectrum. However, the range estimation's precision is still limited by the sample of the spectrum, and in the LRFT it is used as a coarse estimation and then up-sampled within a very small range around the rough estimation through the local virtual sampling Fourier transform; therefore, the computational burden and memory required for the LRFT decrease sharply.

In fact, the local virtual sampling Fourier transform is not an additional approximation technique - it simply discards information outside the valid region, for example, the side-lobe information, and the result is an efficient inverse Fourier transform without any iteration [21]. We will present the algorithm of the local virtual sampling Fourier transform together with its theory in detail in what follows.

We define the matrix-form Fourier transform of the N - dimensional signal $s(t)$ as

$$F(U) = E \cdot s(t) \quad (8)$$

where $U = (u_0, \dots, u_{N_B-1})^T$ and N_B is the number of samples in the frequency domain.

$$E = \begin{bmatrix} e^{i2\pi t_0 u_0} & \dots & e^{i2\pi t_k u_0} & \dots & e^{i2\pi t_{N-1} u_0} \\ \dots & \dots & \dots & \dots & \dots \\ e^{i2\pi t_0 u_k} & \dots & e^{i2\pi t_k u_k} & \dots & e^{i2\pi t_{N-1} u_k} \\ \dots & \dots & \dots & \dots & \dots \\ e^{i2\pi t_0 u_{N_B-1}} & \dots & e^{i2\pi t_k u_{N_B-1}} & \dots & e^{i2\pi t_{N-1} u_{N_B-1}} \end{bmatrix} \quad (9)$$

Equation (8) is deduced from the Riemann sum of the continuous Fourier transform, which is also called the matrix-form Fourier transform (MFFT); however, if N_B is equal to N , Equation (8) will be the Discrete Fourier Transform (DFT) of the signal. We define the local virtual frequency sampling in the following according to the definition of the MFFT.

As is well known, a discrete signal in the Fourier domain corresponds to a continuous periodic signal in the spatial domain; therefore, a new sampling strategy is presented to obtain a signal with a higher resolution in the spatial domain, which is a higher sample rate and which is used when we transform the signal from the frequency to the spatial domain.

Given the virtual sampled region size m (usually $1 \leq m < 2$), the virtual sampling scale k , and the rough estimation of the PC spectrum's peak location t_M (which can be estimated

by the traditional FFT-based method), then the resampling vector R is constructed in the region as

$$R = \left\{ t_M - \frac{m}{2}, t_M - \frac{m}{2} + 1/k, \dots, t_M + \frac{m}{2} \right\} \quad (10)$$

where $1/k < 1$ is the sample step of t' ($k > 1$, set by the user). The region R is the uncertainty interval of the rough range estimation; therefore, the support of the PC spectrum is restricted by the local virtual sampling technique. Furthermore, the peak location's truth might be anywhere within R .

The construction of the base function is the most important part of the local virtual sample in the PC spectrum, as shown in Equation (9). The virtual sample region is set on the basis of m after t_M is estimated. To construct the sample vector T in the spatial domain, we resample R with a $1/k$ origin step. Next, based on the MFFT, the base function is constructed according to the variable $[T, U]$, as shown in Equation (10), to transform the signal from a frequency to the space domain.

$$E_t = \left[e^{i2\pi t_0 u_0} \quad e^{i2\pi t_1 u_1} \quad \dots \quad e^{i2\pi t_{N-1} u_{N-1}} \right]^T \quad (11)$$

As such, we define the local virtual sample of the PC spectrum $P_{hs}(u)$ on R as

$$\begin{cases} \begin{bmatrix} e^{i2\pi t_0 u_0} & \dots & e^{i2\pi t_k u_0} & \dots & e^{i2\pi t_{N_C-1} u_0} \\ \dots & \dots & \dots & \dots & \dots \\ e^{i2\pi t_0 u_k} & \dots & e^{i2\pi t_k u_k} & \dots & e^{i2\pi t_{N_C-1} u_k} \\ \dots & \dots & \dots & \dots & \dots \\ e^{i2\pi t_0 u_{N-1}} & \dots & e^{i2\pi t_k u_{N-1}} & \dots & e^{i2\pi t_{N_C-1} u_{N-1}} \end{bmatrix} \cdot P_{hs}(u) & T' \in R \\ 0 & T' \notin R \end{cases} \quad (12)$$

where $T' = (t_0, t_1, \dots, t_{N_C-1})$ is the resampled spatial variable of the local virtual sample and N_C is the number of samples in the space domain.

The conventional DFT requires that N_C ($N_C = k \cdot m$) is equal to N and that $du/dt = N^{-1}$ (usually m is set in the region $[1, 2]$, du is the frequency domain step and dt is the spatial variable step). However, N_C is always unequal to N , especially in the local virtual sample Fourier transform. Therefore, neither the DFT nor the FFT can be substituted in Equation (8).

To estimate the target range, the PC spectrum of $s(t)$ - which is the echo signal of the radar - and the impulse response $h(t)$ of the matched filter is constructed according to Equation (2). Next, a Dirac delta function is achieved by the inverse Fourier transformation of the PC spectrum, whose peak location is denoted by d_0' such that d_0 is considered to

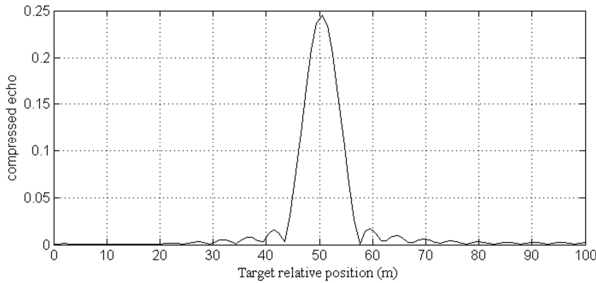
be the initial rough estimate of the range through the traditional FFT-based signal correlation algorithm. Furthermore, the PC spectrum is resampled virtually in a small region around d_0 and then we achieve high accuracy in the local PC spectrum $p(T')$ through the local virtual sample Fourier transform algorithm shown in Equation (12). The location of its peak, denoted by Δd_0 , which is shown in Equation (13), is the amended parameter of the range to d_0 and at last a more accurate estimation of the range is achieved by Equation (14),

$$\Delta d_0 = \arg \max(p(T')) \quad (13)$$

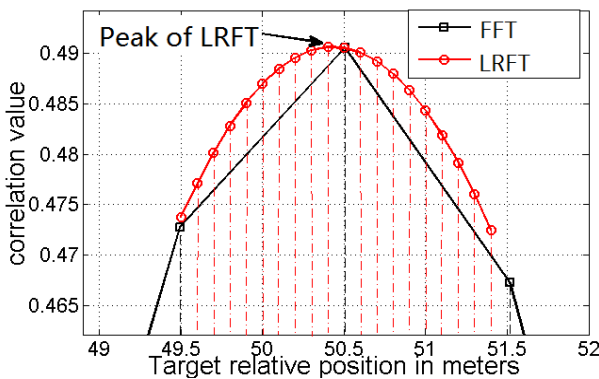
$$d = d_0 + \Delta d_0 \quad (14)$$

where d is the estimated target range detected by the radar. This method is the LRFT for the target range estimation.

Fig. 3(a) shows a receive-window PC spectrum achieved by the conventional FFT method. The peak location of the spectrum, which is shown in Fig. 3(b) in detail, corresponds to the rough range estimation. A more accurate range estimation cannot be achieved by this method. The virtual sample PC spectrum is described by the red line in Fig. 3(b), and the black line is part of the traditional FFT-based PC spectrum around its peak. From the comparison, it can be concluded that the LRFT spectrum's peak location is more accurate.



(a) A traditional PC spectrum achieved by the FFT method



(b) The LRFT spectrum (red)

Figure 3. Spectrum of PC and the LRFT ($m=2, k=10$)

4. Experimental results and discussion

In this section, we present the experimental validation of the algorithm's performance on synthesis data and a physical system, and the efficiency analysis of the LRFT for radar range estimation is also introduced.

4.1 Experiments on synthesis data

Firstly, the precision experiments for the LRFT algorithm are introduced. Next, our method is compared with traditional FFT-based PC. Finally, we introduce the computational time of the LRFT. We validate the LRFT method in MATLAB 2009b, running on a Pentium IV 2.8 GHz Intel CPU with 1,024 Mb memory.

The range estimation precision of the LRFT is validated at different bandwidths, and the parameters of the simulated radar are as follows: the receive-window size is 500 m, the scatters RCS is 1 m², and the bandwidth changes from 10 MHz to 100 MHz. The resample step k in the LRFT is set to 10. We test the range estimate precision at each bandwidth setting for scatter ranges from 10 m to 750 m with 25 m steps, and we then average the range estimate error corresponding to the bandwidth. Table 1 shows the experimental results.

Bandwidth h (MHz)	10	20	30	40	50	60	70	80	90	100
Range error (m)	0.306	0.131	0.084	0.058	0.046	0.037	0.031	0.029	0.025	0.022

Table 1. Averaged estimation error of the LRFT corresponding to different bandwidths

It can be seen in Table 1 that even if the bandwidth is narrow - such as 10 MHz - the range is still estimated accurately.

Next, we compare the precision of our LRFT method and the traditional FFT-based PC method. At a given bandwidth, we simulate 10 random scatters and estimate the corresponding 10 range errors separately, and finally the 10 errors are averaged. Figure 4 shows the comparison of the experimental results, and it is found that the range-estimate errors of the LRFT decrease sharply at bandwidths lower than 70 MHz compared with the FFT-based PC method. The parameter p shown in Figure 5, which characterizes the improvement in precision of our method, is defined in Equation (15),

$$p = (e_{FFT} - e_{LRFT}) / e_{FFT} \quad (15)$$

where e_{LRFT} and e_{FFT} describe the range estimation error of our LRFT method and the traditional FFT-based method, respectively.

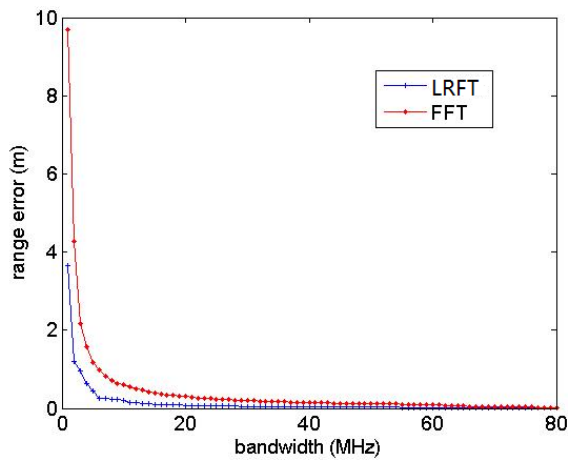


Figure 4. Range estimation comparison between the FFT-based method and our LRFT method

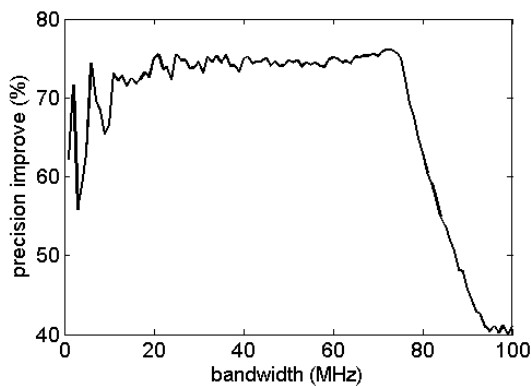


Figure 5. The range estimation precision improvement of the LRFT compared with the traditional FFT method

At the same time, the robustness of the LRFT is validated, Gaussian white noise is added to the echo signals. For every bandwidth, 50 times Monte Carlo experiments are designed with random noise of SNR from -20 dB to -5 dB tested then the range estimation errors are averaged. The results are shown in Table 2, from which it can be seen that the LRFT method achieves greater accuracy than the conventional FFT-based method when disturbed by Gaussian white noise, and from the improvement in precision p it can be seen that the accuracy is improved by more than 35% at the lower bandwidth.

Bandwidth (MHz)	10	20	30	40	50
FFT-based method (m)	17.5	4.2	3.5	1.9	1.4
LRFT (m)	6.5	2.3	1.5	1.2	0.8
Accuracy improvement p (%)	62.9	45.2	57.1	36.8	42.9

Table 2. Range estimation errors of the LRFT and the FFT-based method

The experiments show that we achieve a more precise range estimation using the LRFT method, especially when the radar works at lower bandwidths, and we can get more than 60% improvement in precision (lower than 80 MHz)

compared with the traditional FFT-based PC method. Furthermore, the statistical average time for each range estimation is about 0.6 ms and 0.7 ms for the FFT-based method and the LRFT, respectively, which concurs with the analysis in [21] such that, compared with most FFT-based methods, the local virtual sample technique does not significantly increase the computational burden.

4.2 Experiments on a physical system

Our algorithm was tested on the physical radar system described in Section 2 to validate the performance for accurate range estimation. The parameters of our radar are shown in Table 3 in detail.

Parameter	Symbol	Min.	Typ.	Max.	Units
transmit frequencies*	f_c	24.000	-	24.250	GHz
varactor tuning voltage	V_{tune}	0	-	3	V
tuning slope coarse		-	640	-	MHz/V
tuning slope medium		-	130	-	MHz/V
tuning slope fine		-	40	-	MHz/V
output power (EIRP)	P_{out}	-	20	-	dBm
IF-amplifier	Gain	-	20	-	dB
	Bandwidth	20	-	500k	Hz
T_x - full beam width @ -3dB	Horizontal	-	23	-	°
R_x - full beam width @ -3dB	Horizontal	-	55	-	°

* depending on V_{tune}

Table 3. The detailed parameters of our 24 GHz IVQ-905 radar

We conducted an experiment in a field test for a pedestrian detection and positioning scenario to obtain accurate measurement results and assess our algorithm's ranging precision.

In this experiment, the radar has a central frequency $f_c = 24$ GHz and a bandwidth of $B = 100$ MHz, the sweep time is $T_{sweep} = 0.1$ ms, and there is a three-beat frequency in one measurement cycle. In our experiment, there is a moving pedestrian who is running at the front of the radar, and our proposed LRFT algorithm is used following the received signal de-chirp process. The target measurement scenario is shown in Fig. 6.

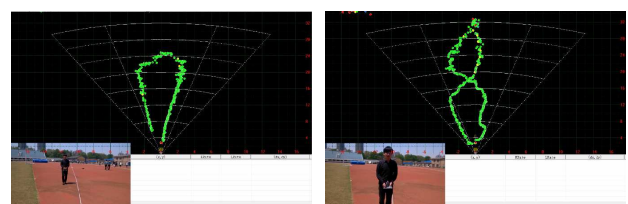


Figure 6. MMW radar target measurement scenario in the field test

To demonstrate the functionality of the algorithm, a quantitative evaluation is performed to analyse the precision for the ranging, and we compare the LRFT algorithm for range enhancement, such that there is about a 30% improvement overall.

5. Conclusion

Automotive MMW radars offer - in general - the capability to measure extremely accurately the target range, radial velocity and azimuth angle for all objects inside the observation area of intelligent vehicles or mobile robots. In this paper, a novel LRFT method for automotive MMW radar range estimation is developed. The LRFT is a method based on a local virtual sample of the PC spectrum in a phase space, which uses a matrix local resample Fourier Transform to achieve virtual resampling in a local neighbourhood of the PC spectrum and estimate the range accurately. From the synthesis data experiments, it was found that we can achieve more accurate estimations compared with the traditional FFT-based method, especially at lower bandwidths. Furthermore, physical radar system experiments have shown the application of our method to pedestrian detection and positioning.

6. Acknowledgements

This work was partially supported by a fund from the National 863 High Technology Research Fund (2015AA8106043), the National Science Foundation of China (Grant No.61402237, 61302156), the Foundation of Nanjing University of Posts and Telecommunication (Grant No. NY212026, and NY213168), and the Jiangsu Key Laboratory of Image and Video Understanding for Social Safety (Nanjing University of Science and Technology - Grant No. 30920140122007).

7. References

- [1] Stove A.G. Linear FMCW radar techniques. IEE Proceedings-F Radar, Sonar Navigation. 1992; 139(5): 343–350.
- [2] Rohling H. Milestones in radar and the success story of automotive radar systems. In 11th International Radar Symposium, Vilnius, 16–18 June 2010, pp. 1–6.
- [3] Massen J., Frei M., Möller W.M.U., Frei M., Menzel W., Möller A.U. A 79 GHz SiGe short-range radar sensor for automotive applications. *Int. J. Microw. Wireless Technol.* 2013; 5(1): 5–14.
- [4] Dzvonkovskaya A.L., Gurgel K.W., Rohling H., Schlick T. HF radar WERA application for ship detection and tracking. *Eur. J. Navigation.* 2009; 7(3): 18–25.
- [5] Clark S., Perletta L. ClearWay radar for the detection and enforcement of illegal vehicle lane change and tail-gating events. In 19th ITS World Congress, Vienna, 22–26 Oct. 2012.
- [6] Fulvio G. Antonio D. M. and Lee K. Patton. *Waveform Design and Diversity for Advanced Radar Systems*, London: The Institution of Engineering and Technology. 2012, pp. 173–205.
- [7] Li G., Meng H., Xia X., Peng Y. Range and velocity estimation of moving targets using multiple stepped-frequency pulse trains. *Sensors.* 2008; 2008(8): 1343-1350.
- [8] Dong W., Zhou Z., Ni X. Application of linear frequency modulation pulse compression in air-coupled ultrasonic testing. In proceeding of Advanced Computer Control. 2010; 2: 53-57.
- [9] Hyun E., Lee J. Method to improve range and velocity error using de-interleaving and frequency interpolation for automotive FMCW radars. *International Journal of Signal Processing Image Processing and Pattern Recognition.* 2009; 2(2): 11-22.
- [10] Song M., Lim J., Shin D. Enhancing Doppler estimation via Newton interpolation for automotive FMCW radar. 2014 International Conference on Information and Communication Technology Convergence (ICTC), pp. 615-616, 2014.
- [11] Qi G. High accuracy range estimation of FMCW level radar based on the phase of the zero-padded FFT. *Proceedings of IEEE International Conference on Signal Processing 2004 (ICSP 2004)*, pp. 2078-2081, 2004.
- [12] Scherr S., Ayhan S., Hofmann J., Pauli M., Zwick T. Sweep time variation algorithm for high accuracy FMCW radar measurements. 2015 German Conference on Microwave (GeMiC), pp. 182-185, 2015.
- [13] Hao, C., Orlando, D., Foglia, G., Ma X.. Adaptive radar detection and range estimation with over-sampled data for partially homogeneous environment. *Signal Processing Letters.* 2015; 22(9): 325-329.
- [14] IVQ-905 datasheet [Internet]; Available from: <http://www.innosent.de/fileadmin/media/dokumente/datasheets/IVQ-905.pdf>. Accessed on 09 Sep 2015.
- [15] Mahafza R.B., Elsherbeni A. *MATLAB Simulations for Radar Systems Design*. Chapman and Hall/CRC; 2003.
- [16] Bucci N.J., Owen H.S., Woodward K.A., Hawes C.M. Validation of pulse compression techniques for meteorological functions. *IEEE Trans. Geosci. Remote Sensing.* 1997; 35(3): 507-523.
- [17] Qi G., Li X., Tian Y. Range estimation accuracy analysis of the FMCW level radar. *International Conference on Signal Processing.* 2006; 4: 2669-2672.
- [18] Wang Y., Wang W., Shao H. Frequency diverse array radar Cramér-Rao lower bounds for estimating direction, range, and velocity. *International Journal of Antennas and Propagation.* 2014; 2014: 1-15.
- [19] Tshe, S., Purik, D. Han S.H. Range resolution improvement of pulse compression radar. In

International Asia-Pacific Conference on Synthetic Aperture Radar (APSAR); 2011, pp. 1-4.

- [20] Yang S., Cheng K., Wang M., Xie D., Jiao L. High resolution range-reflectivity estimation of radar targets via compressive sampling and Memetic. *Algorithm Information Sciences*. 2013; 252: 144-156.

- [21] Wang C., Jing X., Zhao C. Local upsampling Fourier transform for accurate 2D/3D image registration. *Computer and Electrical Engineering*. 2012; 38: 1346-1357.